Cavity Ring-Down Laser Absorption Spectroscopy of Jet-Cooled L-Tryptophan

Gaël Rouillé,[†] Marco Arold,[†] Angela Staicu,[‡] Thomas Henning,[†] and Friedrich Huisken*,[†]

Laboratory Astrophysics Group of the Max Planck Institute for Astronomy at the Friedrich Schiller University Jena, Institute of Solid State Physics, Helmholtzweg 3, D-07743 Jena, Germany, and National Institute for Lasers, Plasma and Radiation Physics, Laser Department, P.O. Box MG-36, 077125 Magurele, Bucharest, Romania

Received: April 8, 2009; Revised Manuscript Received: May 29, 2009

The jet-cooled ultraviolet direct absorption spectrum of the amino acid tryptophan is reported. The spectrum measured by cavity ring-down laser absorption spectroscopy covers the region where the origin bands of the $S_1 \leftarrow S_0$ transitions of six conformers (A to F) are located. Tryptophan was transferred into the gas phase by two different methods, namely, thermal heating and laser vaporization. The latter technique allowed us to obtain higher densities of tryptophan in the jet at the time when it was probed for spectroscopy. It also avoided thermal decomposition of the sample. On the other hand, a higher signal-to-noise ratio was obtained with thermal heating. Measurements were carried out by laser-induced fluorescence as well. The comparison of the absorption and excitation spectra reveals a higher fluorescence yield and a shorter radiative lifetime for the S_1 state of conformer A relative to the other conformers. Moreover, the comparison of our spectra with each other and with literature data led us to assign a band to a new conformer, which we named G. Finally, the theoretical structure and vibrational frequencies obtained from density functional theory based calculations confirm that the progression observed in the $S_1 \leftarrow S_0$ spectrum of conformer A is consistent with a torsional motion of the amino acid side chain relative to the indole chromophore.

Introduction

As organic molecules bearing carboxyl and amino groups have been identified in the circum- and interstellar media, it is conceivable that amino acids are present in space. Quite notably, the observation of microwave emission lines of the amino acid glycine has been reported[1] before being disputed in subsequent publications.[2−4] To date, microwave emission observations have been the major means for detecting and identifying interstellar molecules. Progresses in microwave observational techniques, however, are such that the confusion limit is almost reached. It becomes attractive to explore other wavelength ranges. For instance, using background stars as light sources, molecules could be identified by the analysis of their electronic absorption spectra in the ultraviolet (UV) wavelength range. In order to proceed with the spectroscopic identification of circum- and interstellar molecules, reference absorption spectra have to be measured in the laboratory under conditions similar to those found in the relevant regions.

The amino acid tryptophan (Trp) is an interesting candidate for an interstellar search. It is a chiral molecule containing an indole chromophore of high fluorescence yield. One enantiomer, L-tryptophan, is a component of proteins and belongs to one of our essential amino acids. It is used as a fluorescent probe in processes involving proteins, justifying numerous studies in solutions. Spectroscopic studies in supersonic jets and molecular beams, nevertheless, have been carried out with the aim to better understand the intrinsic photophysics of the molecule. One color 1 + 1 resonance-enhanced multiphoton ionization (R2PI),[5−8] laser-induced fluorescence (LIF),[6,9,10] ionization-detected UV−UV hole burning,[7,8] and ionization-detected IR-UV hole burning[8] have been employed for that purpose. Six conformers, labeled A to F, were identified.[5,7,8]

Until now, the vibrationally excited states of Trp have been studied using techniques that took advantage of secondary processes arising from the one-photon absorption. Because the yields of the secondary processes as a function of the vibronic states are unknown, one cannot determine the one-photon absorption intensities from these measurements. This is particularly true if different conformers contribute to the spectrum.

In order to obtain data of relevance to astronomy, we report in this paper jet-cooled absorption spectra of Trp in the region of the $S_1 \leftarrow S_0$ origin bands of the known conformers A to F. These direct absorption measurements have been carried out with the cavity ring-down laser absorption spectroscopy (CRDS) technique. Moreover, we have also measured LIF spectra of Trp in the same range and under similar conditions to reveal the differences between the direct absorption and excitation spectra. As a consequence, we were able to determine the fluorescence yields and nonradiative rate coefficients of the different conformers. The new data also allowed us to assign a band to a new conformer, labeled G, and to reach new conclusions concerning the photophysics of Trp. Finally, density functional theory (DFT) based calculations were used to obtain the theoretical structure and vibrational frequencies for the S_0 state of the conformer A of Trp. The low-energy vibrational progression in the $S_1 \leftarrow S_0$ spectrum of conformer A is compared with calculated frequencies for the first time. The vibrational progression of conformer A is assigned to a torsional motion of the amino acid side chain relative to the indole chromophore.

Experimental Methods

Transfer of Tryptophan into the Gas Phase. In the solid phase, Trp is in the form of a zwitterion. The initial temperature of decomposition lies in the range 270−277 °C.[11] When heated to such temperatures, Trp decomposes in a decarboxylation

* Corresponding author. E-mail: friedrich.huisken@uni-jena.de.
[†] Max Planck Institute for Astronomy and Friedrich Schiller University Jena.
[‡] National Institute for Lasers, Plasma and Radiation Physics at Bucharest.

10.1021/jp903253s CCC: $40.75
Published on Web 07/01/2009

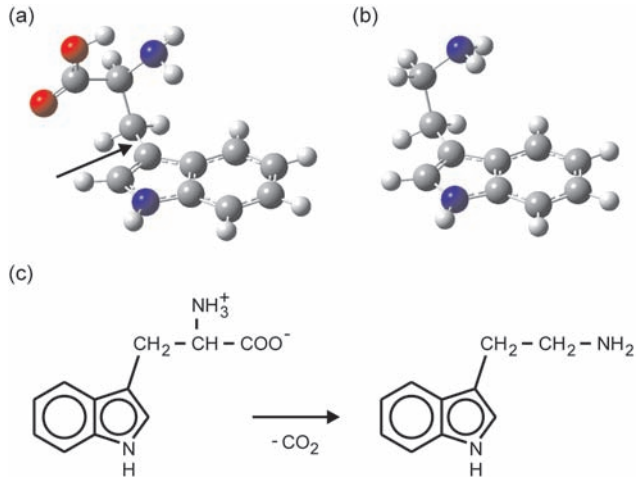

Figure 1. (a) Conformer A of L-tryptophan. The arrow points at the CC bond that connects the amino acid side chain with the indole chromophore. (b) Conformer F of tryptamine. The geometries have been optimized at the DFT-B3LYP/6-31+G(d,p) level based on the results of Snoek et al.[8] for Trp and Schmitt et al.[32] for tryptamine. The calculations were carried out with the Gaussian software.[29] (c) Decarboxylation of the zwitterionic form of tryptophan in the solid phase according to ref 12.

reaction which yields tryptamine, as described by differential enthalpic analysis[12] and confirmed by mass spectrometry measurements.[5] Figure 1 shows the structures of Trp and tryptamine and a schematic of the decarboxylation of the Trp zwitterion. Different procedures of thermal heating were designed to transfer the molecule into the gas phase while minimizing thermal decomposition.[5,9,10] Besides the procedures based on thermal heating, matrix-assisted laser desorption was also employed.[7] This technique is a particular case of what is termed laser vaporization, which is the transformation of a condensed sample into a vapor by a thermal process induced by the interaction with a laser beam.[13] We have implemented both techniques in order to compare their efficiencies. In either case, the sample was L-tryptophan (Fluka, purity ≥99.5%).

Thermal heating has been applied to the pure sample powder contained in a small aluminum reservoir placed inside a heated pulsed valve which we have already described.[14,15] It consists of a commercial solenoid valve (General Valve series 9) to which a small chamber containing the sample was attached. This sample chamber, equipped with a nozzle of 1 mm diameter, can be heated up to 500 °C with a stability of 1 °C. All measurements on thermally vaporized Trp presented in this work were carried out in the 200−300 °C range with helium (Linde, 99.999% purity) as the carrier gas and a backing pressure of 1.5 bar. Argon was dismissed for that purpose after we had observed strong broad features in the absorption spectrum of Trp, possibly caused by complexes of Trp with Ar. The heated valve was operated to produce gas jets with a duration of 600 μs at a repetition rate of 20 Hz.

The source which we have used for laser vaporization is similar to that described by Piuzzi et al.[7] Originally in the form of a powder, the sample was pressed to produce a 2 mm thick pellet which was cut to obtain pieces with straight edges. The two pieces were mounted end to end on a motorized stage as close as possible to the 0.8 mm diameter nozzle exit of a pulsed valve (General Valve series 9). As the valve opens, a carrier gas, in that instance Ar, with a backing pressure of 1.5 bar, expands adiabatically above the surface of the sample. Although the formation of complexes was observed when using the heated valve with Ar as the carrier gas, it was not under these new conditions since the molecules were injected into the carrier gas after it started to expand. Each time the valve opens, the focused beam from a quadrupled (λ = 266 nm) pulsed Nd:YAG laser (Continuum Minilite) hits the sample at a point aligned with the nozzle axis. This point and the nozzle exit are separated by 1 mm. Molecules are then thermally desorbed and ejected into the expanding carrier gas where they are to be probed by CRDS. Although the laser pulse has a duration of 7 ns, we have observed that the vaporization process lasts several microseconds after the laser beam has hit the sample, confirming the thermal nature of the process and enabling us to apply the CRDS technique. In terms of signal-to-noise ratio, the best results have been obtained by analyzing a portion of the decay signal which had a 3.4 μs duration. Consecutive laser shots did not hit the sample at the same point as it was continuously translated on the motorized mount without any synchronization with the valve. A rotatable Glan−Taylor prism in the path of the beam was used to adjust the laser fluence.

Cavity Ring-Down Laser Absorption Spectroscopy. A detailed description of the cavity ring-down laser absorption spectrometer has been published previously.[14−16] The laser source was a tunable dye laser (Continuum ND6000) pumped by a pulsed Nd:YAG laser (Continuum Surelite II-20) with a pulse duration of 5 ns. The dye laser oscillator was equipped with a single grating of 2400 lines per millimeter. We used rhodamine 6G (Lambda Physik LC5900) dissolved in methanol as laser dye.

The yellow beam emitted by the dye laser was frequency-doubled by means of a KD*P crystal (Continuum DCC3), the orientation of which was optimized by a tracking system. The resulting ultraviolet beam was injected into the 1 m long cavity formed by a pair of identical high-reflectance concave mirrors with a radius of curvature of 6 m (Japan Aviation Electronics). A reflectance of at least 0.99978 at 286.5 nm was determined by measuring a decay time of 15.2 μs when the molecular beam chamber was evacuated. In order to block the stray light at the visible fundamental wavelength emitted by the dye laser, the photomultiplier module detector (Hamamatsu H6780−04) placed behind the exit mirror was protected by a color filter (Schott UG11).

The laser line width was estimated to be 0.256 cm^{-1} at 572.08 nm by fitting a Lorentzian to the profile of a NeI absorption line observed in a hollow cathode lamp (Hamamatsu L233−26NU). This value represents an upper limit since it actually includes the contribution of the intrinsic width of the NeI line. The wavelength calibration of the laser was performed by measuring the positions of several NeI lines in the 565 to 577 nm range.[17] Moreover, the absorption spectrum of NeI was recorded simultaneously with the spectra of Trp. As a result, the resulting uncertainty of the wavenumber scale is smaller than 0.05 cm^{-1} relative to the NeI line positions. Thus, we assume an uncertainty of 0.1 cm^{-1} in the range of the doubled frequency. All wavenumbers and wavelengths reported in this work are given for vacuum.

The presented CRDS spectra report the absorbance A of the Trp-seeded jet. It is defined as the product of three parameters which are the number of absorbing molecules per unit volume in the jet, the molecular absorption cross section, and the diameter of the jet. It is obtained from the measured decay time of the CRDS signal, τ, through the relation

$$A = \frac{L_c}{c\tau} + \ln R \quad (1)$$

where L_c is the length of the cavity, c the speed of light in vacuum, and R the reflectance of the mirrors. The nonresonant background signal associated with the reflectance of the cavity mirrors and the scattering losses caused by the gas jet was subtracted from the spectra.

Laser-Induced Fluorescence Spectroscopy. The CRDS setup also allowed us, with little modifications, to perform LIF spectroscopy. The high-reflectance mirrors were replaced by windows set at Brewster angle. The pinhole and lens arrangement was kept to provide a collimated laser beam of 2 mm diameter with low intensity. Photons emitted from the region where the laser beam crossed the molecular beam axis were collected at right angles to both the laser beam and the gas jet axes. The collecting optics was a quartz lens with a diameter of 50 mm and a focal length of 44 mm. A second lens of the same diameter, but with a focal length of 200 mm, slightly focused the collected fluorescence through a quartz window onto the photocathode of a photomultiplier tube (THORN EMI 9813QB). In the range from 200 to 460 nm, the quantum efficiency of the photocathode varies between 22% and 26%, and it decreases quickly beyond 460 nm. In the present work, no filters were used for wavelength selection. A gated integrator (Stanford Research Systems SR250) measured the fluorescence intensity. The wavelength calibration was made following the same procedure as that used for the CRDS measurements.

Results

CRDS with the Heated Valve. Figure 2 shows absorption spectra of Trp as the gas jet was probed 4 mm downstream from the nozzle exit. Each point in the spectra, taken at 0.005 nm intervals, represents the average of 64 measurements. This wavelength interval corresponds to 0.6 cm^{-1} at 35 000 cm^{-1}, a value larger than the laser line width. The $S_1 \leftarrow S_0$ origin bands of Trp are labeled with the characters A to F depending on the conformers they are assigned to. Only for conformer A, which exhibits a vibrational progression, initial and final vibrational quantum numbers are indicated. The spectra were recorded consecutively from bottom to top as the heating element of the valve was adjusted to 261, 267, and 270 °C, with two scans carried out at 270 °C. Features such as band shapes and relative intensities are well-reproduced in the consecutive scans, and the growth of the absorption bands attributed to the conformers of Trp as a function of the source temperature is clearly noticed. In the second spectrum recorded with the source temperature of 270 °C, the bands of Trp have the same intensity as in the first one. Some bands denoted with asterisks in Figure 2 behave differently from those of the amino acid. The intensity of these bands, the strongest of which lies at 34 916 cm^{-1}, keeps increasing although the temperature of the source is constant. These bands are attributed to those of tryptamine.

We have already mentioned that Trp is subject to thermal decomposition, with tryptamine as the main product.[5,12] This molecule exhibits absorption bands in the region where the origin bands of the different Trp conformers are found. In order to identify them, we have also recorded the absorption spectrum of pure tryptamine (Sigma, purity ≥99%) within the wavelength range of interest. (The spectrum is shown in Figure 4a.) It was obtained by keeping the heating element of the valve at 144 °C and probing the jet 4 mm downstream from the nozzle exit. The absorption spectrum of tryptamine is similar to the two-

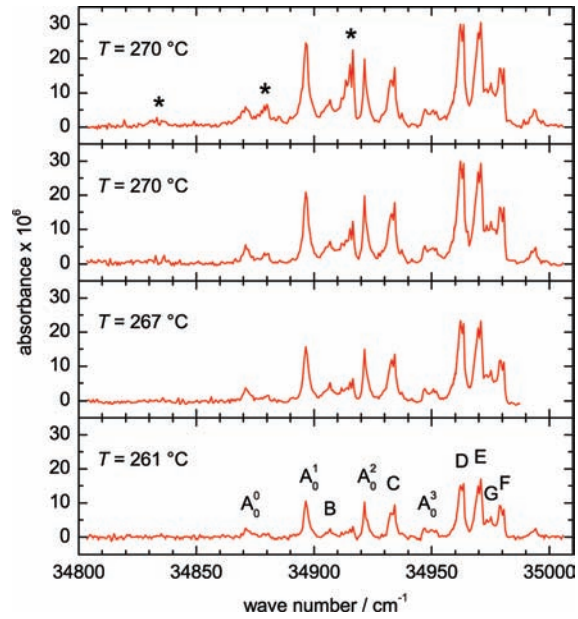

Figure 2. From bottom to top: $S_1 \leftarrow S_0$ CRDS absorption spectra of L-tryptophan vaporized in a heated valve at different temperatures and cooled in a supersonic jet. The bands are labeled according to the conformers to which they are attributed, while bands of tryptamine are indicated by asterisks. The absorbance of the jet increases with the temperature of the source. When it is kept constant at 270 °C, bands due to Trp do not evolve while those due to tryptamine keep growing in intensity.

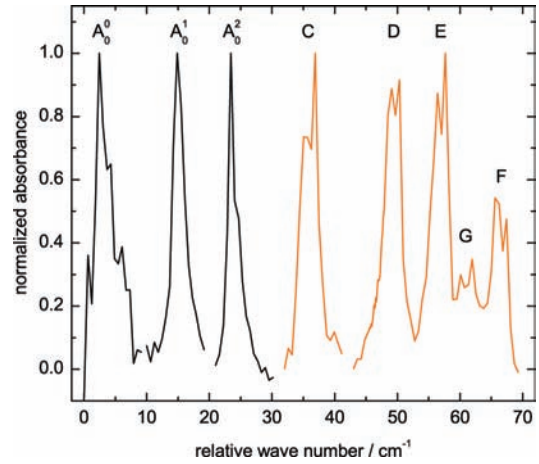

Figure 3. Enlarged view of the band contours in the jet-cooled absorption spectrum of Trp. The bands are taken from the spectrum in Figure 2 that was observed with a source temperature of 261 °C. The weak bands A_0^3 and B are not included.

photon ionization and LIF spectra of this compound reported by Park et al.[18] and by Philips and Levy,[19] respectively.

As can be seen in Figure 2, the absorption spectrum of conformer A of Trp differs from those of the other conformers in two respects. First, as known from LIF and R2PI studies, the spectrum of conformer A exhibits a vibrational progression with a separation of 26 cm^{-1},[5,6] a value which we presently estimate to be closer to 25.5 cm^{-1}. According to ref 5, the intensity pattern in this progression indicates "a significant geometry change in the coordinate of this vibration upon electronic excitation". Second, it was not yet reported that the rotational contours of the bands belonging to conformer A show a single peak as illustrated in Figure 3. They are steeper on the low-energy side and have a full width at half-maximum (fwhm) of the order of 2 cm^{-1}. By contrast, the contours of the bands

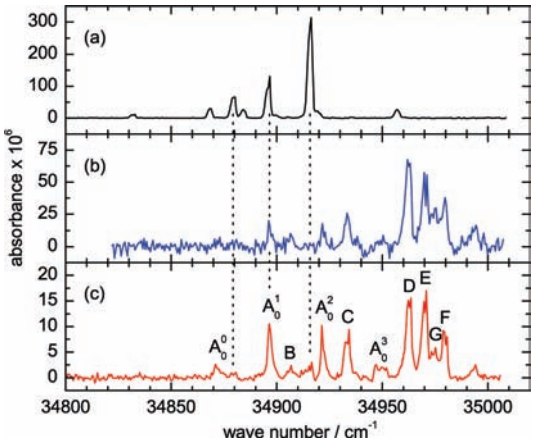

Figure 4. (a) Absorption spectrum of jet-cooled tryptamine measured for reference. (b) Jet-cooled absorption spectrum of Trp obtained with laser vaporization. (c) Jet-cooled absorption spectrum of Trp obtained with the sample placed into the heated valve at 261 °C (same spectrum as in Figure 2). Dashed lines mark the positions of the strongest bands of tryptamine in the Trp spectra.

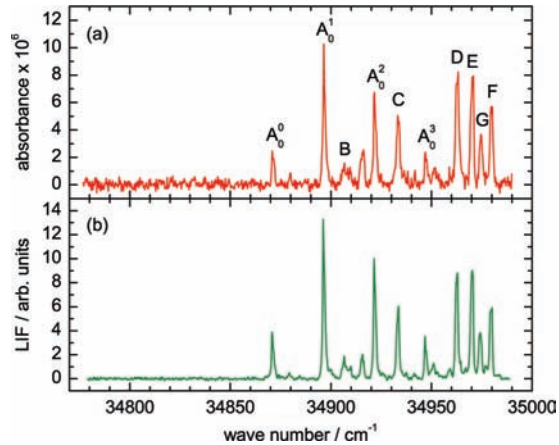

Figure 5. (a) Jet-cooled absorption spectrum of Trp obtained with the sample placed into the heated valve at 292 °C and by probing the jet 14 mm downstream from the source. (b) Laser-induced fluorescence spectrum of Trp obtained with the same experimental parameters.

related to the other conformers show two peaks which correspond to rotational P and R branches. They are steeper on the high-energy side and have a significantly larger fwhm of the order of 3.5 cm^{-1}.

CRDS with Laser Vaporization. The absorption spectrum of Trp transferred to the gas phase by laser vaporization is shown in Figure 4b. In order to obtain the same vaporization conditions as those used by Piuzzi et al.,[7] we first tried to work with a sample of Trp mixed with graphite and with a vaporization laser wavelength of 532 nm. In this situation, graphite absorbs the green photons and converts their energy into thermal heat which is transferred to the Trp crystallites, causing their vaporization. Under such conditions, we did not observe absorption bands, a result attributable to the lower sensitivity of CRDS compared with that of the photoionization spectroscopy technique used by Piuzzi et al.[7] The present spectrum has been obtained with a pure Trp sample and a vaporization wavelength of 266 nm, which is more adapted to the absorption behavior of solid Trp than 532 nm.[20,21] We estimate the fluence to be 17 mJ cm^{-2} at the surface of the pellet where the laser beam formed a spot of 0.3 mm diameter. It is an order of magnitude lower than the threshold above which significant amounts of ions are produced.[20] The gas jet was probed 4 mm downstream from the vaporization point. Improvement in signal size and quality can be immediately noticed when comparing the as-obtained spectrum with the one shown in Figure 4c, which was obtained with the heated valve. First, a higher absorbance is reached, indicating a higher density of Trp in the jet during the time necessary for measuring the time constant of the CRDS signal. Second, tryptamine bands are not observed, even after working for a long time. On the other hand, the signal-to-noise ratio is lower although the signal was averaged 4 times longer than for spectrum Figure 4c. We attribute this lower signal-to-noise ratio to the combination of two effects. The first source of noise is the larger variation of the Trp density in the jet from shot to shot. The CRDS technique measures both the absorption and the scattering that are due to the molecules. As the scattering contributes to the spectra as a significant nonresonant signal, the signal-to-noise ratio of the baseline is also affected. It could be that ablated particles or clusters formed during the vaporization also contribute to this noise. The second factor concerns the time during which the decay is measured. With laser vaporization, the best signal-to-noise ratio was obtained when the decay was measured over a 3.4 μs long portion of the decay curve. We interpret this as the consequence of a vaporization process with a short duration of the order of a few microseconds.[22] In contrast, with the heated valve, the decay was evaluated over a 34 μs long portion of the decay curve. Both the durable presence of Trp in the jet and the high reflectance of the mirrors made this possible. As a consequence, the decay was more accurately determined, and the signal-to-noise ratio was higher than with laser vaporization.

LIF with the Heated Valve. For a proper comparison of excitation and direct absorption measurements, LIF and CRDS spectra have been recorded under identical conditions. In either case, the heating element of the valve was kept at 292 °C, the carrier gas was He with a backing pressure of 1.5 bar, and the Trp-seeded jet was probed 14 mm downstream from the nozzle exit. This distance was chosen in order to minimize the signal arising from the scattered light. In spite of such precaution, the LIF signal, which originates from states with lifetimes on the order of 12 ns,[9,10] had to be measured superimposed on a scattered light signal. Data were acquired at 0.0025 nm intervals in both cases, with averagings over 30 and 64 laser shots for LIF and CRDS measurements, respectively.

The spectra are displayed in Figure 5. As in the CRDS spectra of Figure 2, the difference between the fwhm of the bands of conformer A and those of the other conformers is noticeable, despite the narrower band profiles caused by the lower rotational temperature in the probed region. Since the signal-to-noise ratio is higher in the LIF spectrum than in the CRDS spectrum, we have chosen to use the LIF measurements to determine the band positions. Accordingly, Table 1 contains the positions determined by fitting Lorentzian profiles to the bands in the LIF spectrum. The values we have found are 2 to 3 cm^{-1} lower than those reported by Rizzo et al.[5]

Discussion

Thermal Heating vs Laser Vaporization. We want to examine the absorption spectra for differences arising from the chosen vaporization technique. Laser vaporization was originally introduced in mass spectrometry to transfer nonvolatile and thermally labile species from the solid state into the gas phase without decomposing them.[23] The technique was later applied to optical spectroscopy in molecular beams and supersonic jets.[24,25] Experimentally, we observed the growth of tryptamine bands over time when using the heated valve, whereas we could

TABLE 1: Measured Band Positions and Shifts in the $S_1 \leftarrow S_0$ LIF Spectrum of Jet-Cooled Trp Where All Values are Expressed in Units of cm^{-1} and Given for Vacuum

band position	accuracy	shift	shift[a]	assignment
34 870.95	0.13	0	0	A_0^0
34 896.40	0.12	25.45	26.3	A_0^1
34 906.56	0.17	35.61	35.9	B
34 921.68	0.13	50.73	51.3	A_0^2
34 933.35	0.13	62.40	63.3	C
34 946.91	0.14	75.96	76.7	A_0^3
34 950.99	0.26	80.04	82.6	δ^b
34 962.58	0.14	91.63	91.8	D
34 970.11	0.14	99.16	99.5	E
		101.05[c]	103.4	A_0^4
34 974.23	0.18	103.28		G
34 979.61	0.15	108.66	109.2	F

[a] Values reported by Rizzo et al.[5] relative to their measured A_0^0 band position at 34 873 cm^{-1}. [b] Label for this band of conformer A in ref 8. [c] Predicted, this work.

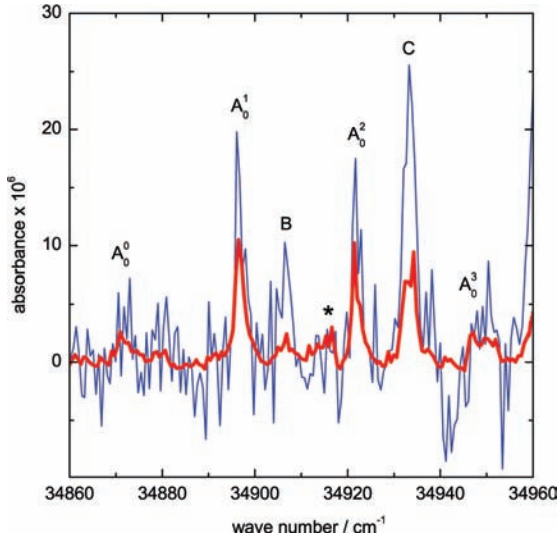

Figure 6. Close-up of the CRDS spectra of Trp displayed in Figure 4b,c which were obtained with laser vaporization (thin line) and thermal heating (thick line), respectively. The asterisk marks a band of tryptamine. Note the change in the intensity of the bands of conformer A relative to the intensity of the band of conformer C if thermal heating is used instead of laser vaporization.

work for hours with laser vaporization without detecting these bands. In the heated valve, the decarboxylation rate of Trp is such that detectable amounts of tryptamine are obtained. Laser vaporization offers the possibility to heat a small volume of the sample for a very short time, preventing the formation of a significant amount of tryptamine. Therefore, higher temperatures can be replaced with increasing the quantity of energy delivered by the laser, and higher densities of vapor molecules can be attained in the jet as shown by the comparison of Figure 4b,c.

A visual inspection of Figure 4b,c reveals that the density of conformer A is significantly larger than the other conformers when we use thermal heating rather than laser vaporization. This observation is particularly striking in the close-up comparison of the two spectra displayed in Figure 6. It should be noted that such a difference also exists between R2PI spectra obtained with thermal heating[6] and laser vaporization.[7] This statement, however, has to be taken with caution since both the thermal heating and the laser vaporization methods implemented in these works were different from ours. Nonetheless, it appears that laser vaporization induces a weakening of the signal from conformer A relative to the signals from the other conformers if compared with thermal heating.

This phenomenon can be explained by the dependence of the relative populations of the conformers on temperature at thermodynamic equilibrium. As the temperature increases, the population of a higher-energy conformer increases relative to that of the lowest-energy conformer. We assume that the molecules reach thermodynamic equilibrium before they are cooled down in the carrier gas expansion irrespective of the vaporization technique used. The relative populations of the conformers are frozen due to fast cooling, provided that the barriers to interconversion are high enough.[26] Although the rotational temperature of the molecules can reach a value of the order of 10 K as observed with jet-cooled anthracene,[14] we consider the relative populations to be characteristic of the temperature reached by the molecules during the vaporization process. This is consistent with the theoretical study of Huang et al. who showed that, if the molecules were at thermodynamic equilibrium, only conformer A would be present for temperatures lower than 85 K.[27] In our experiments with the heated valve, the temperature applied to the sample was higher than 261 °C (see Figure 2). Considering that conformer A is the lowest-energy conformer,[8] the lower intensities of the A bands in the spectra measured with laser vaporization can be explained.

The vaporization temperature should affect the intensities of the bands of all conformers. Examination of the spectra in Figure 4b,c reveals that the bands of conformers C and E are also weakened relative to those of B, D, and F when laser vaporization is used instead of thermal heating, but to a lesser extent. According to the calculations of Snoek et al.,[8] the lowest energy conformer is A. The other conformers form two groups. Relative to the energy of conformer A, conformers E, C, and F have energies in the 4.32−4.54 kJ mol^{-1} range. At even higher energies, one finds conformers D and B with 7.20 and 8.20 kJ mol^{-1}, respectively. We made the assumption that the populations of conformers of similar energies vary in the same way with the temperature. If it was correct, the intensities of the C, E, and F bands should be weakened relative to those of the B and D bands when the temperature is increased. Except for the behavior of conformer F, this correlates with our observations. For a better comparison of the bands, which could contribute to the ordering of the conformers according to their energies, a higher signal-to-noise ratio must be attained when using laser vaporization.

Photophysical Properties. Information on the photophysics of Trp can be obtained from the comparison of the fluorescence and absorption spectra. For a given conformer X (X = A to F), the area of a band in the LIF spectrum, A^X_{LIF}, is proportional to the area of the same band in the CRDS spectrum, A^X_{CRDS}, by

$$A^X_{LIF} = K\phi^X A^X_{CRDS} \quad (2)$$

where ϕ^X is the fluorescence yield of the excited state and K is a factor that takes into account differences between the experiments such as differences in the laser intensity or those in the signal scaling. Equation 2 allows us to determine the fluorescence yield of the excited state of conformer X provided that the value of K is known. Since this value has not been evaluated, the yields can be determined only relative to each other. The yield chosen for reference is that associated with the origin band of conformer A, thus

$$\frac{\phi^X}{\phi^A} = \frac{A^X_{LIF}}{A^X_{CRDS}} \frac{A^A_{CRDS}}{A^A_{LIF}} \tag{3}$$

where the superscript A has been chosen rather than A_0^0 for simplicity.

Since the procedure is only valid if the relative populations of conformers are the same in the fluorescence and absorption spectra, we have calculated the ratios defined in eq 3 by using the band areas obtained from the LIF and CRDS spectra of Figure 5 which were recorded under identical conditions. These spectra are superimposed in Figure 7 where the differences between LIF and CRDS relative intensities are easier to observe. The ratios are plotted in Figure 8. The figure shows that the vibrationless S_1 state of conformer A has a fluorescence yield which is approximately 1.6 times larger than that of the other conformers.

It was found that conformer A behaves differently from the other conformers by showing a stronger contribution of the so-called red-shifted fluorescence.[6,9] Consisting of considerably red-shifted broad bands, it was first interpreted as fluorescence bands from an excited state of a zwitterion form of conformer A.[6] The involvement of a zwitterion form was later invalidated as the red-shifted emission was shown to be the mirror image of the higher energy range of the excitation spectra, with broadened bands.[8,28] We conclude that the lower fluorescence yield in conformers B to F is due to the absence of the radiative deexcitation channel at red-shifted wavelengths which is present in conformer A.

Conformer A also differs from the other conformers by an observed fluorescence lifetime of 10.4 to 10.9 ns in the vibrationless S_1 state, to be compared with 12.8 to 14.5 ns measured for conformers B to F.[9,10] These lifetimes, τ^X_{exc}, correspond to the lifetimes of the excited states which are in fact reduced by nonradiative processes. In the absence of nonradiative deexcitations, one obtains the intrinsic fluorescence lifetime or radiative lifetime, τ^X_{rad}. By considering only two deexcitation processes, radiative and nonradiative deexcitations, the knowledge of the fluorescence lifetimes and the relative fluorescence yields allows us to determine the radiative lifetimes of all conformers relative to that of conformer A by the expression

$$\frac{\tau^X_{rad}}{\tau^A_{rad}} = \frac{\phi^A}{\phi^X} \frac{\tau^X_{exc}}{\tau^A_{exc}} \tag{4}$$

With the excited state lifetimes measured by Teh et al.[10] for each conformer except B, we find with eq 4 $\tau^X_{rad}/\tau^A_{rad}$ ratios of 2.1, 2.3, 2.0, and 2.3 for conformers C to F, respectively. We used the measurements of Philips et al.[9] to determine a $\tau^B_{rad}/\tau^A_{rad}$ ratio of 2.0 for conformer B. The values reported by Philips et al.[9] for conformers A, C, and D are slightly smaller than those reported by Teh et al.[10] for the same conformers. The differences, however, would not affect this discussion in a significant manner. Thus, we have found that the intrinsic fluorescence or radiative rate coefficient k_{rad}, the reciprocal of τ_{rad}, is two times larger in conformer A than in the other conformers.

Philips et al.[9] assumed that all conformers, including conformer A, had the same radiative lifetime and concluded that an additional nonradiative mechanism should be operative in conformer A to explain the shorter lifetime of its excited state. As we have just found that $\tau^A_{rad} \approx \tau^X_{rad}/2$, the assumption made by these authors is therefore not valid and new conclusions

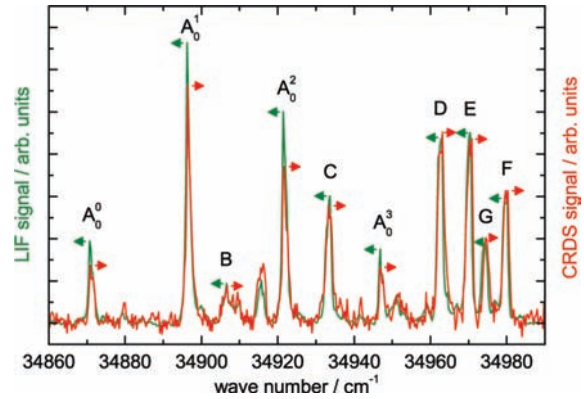

Figure 7. LIF and CRDS spectra of Figure 5 are superimposed for comparison. The spectra were measured under the same conditions. Arrows indicate the maxima of the bands.

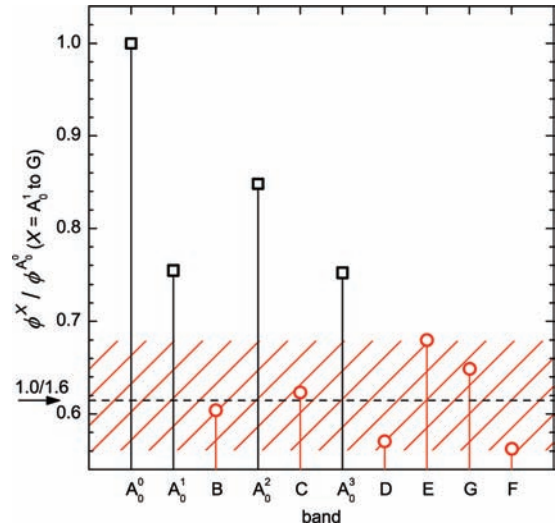

Figure 8. Normalized fluorescence yields obtained by calculating, for each band, the ratio of its area measured in the LIF spectrum to its area measured in the CRDS spectrum (□ conformer A, ○ conformers B to G). The hatched area marks the range where the yields of conformers B to G are found, and their average is indicated by an arrow and a dashed line.

concerning the nonradiative rates should be drawn. The available data allow us to express the nonradiative rate coefficients of conformers B to F, k^X_{nrad}, as linear functions of the nonradiative rate coefficient of conformer A, k^A_{nrad}, such as

$$k^X_{nrad} = \left[\frac{\tau^A_{rad}}{\tau^X_{rad}}\right] k^A_{nrad} + \left[\frac{1}{\tau^X_{exc}} - \left(\frac{\tau^A_{rad}}{\tau^X_{rad}}\right)\frac{1}{\tau^A_{exc}}\right] \tag{5}$$

The nonradiative rate coefficient of conformer A has an upper limit of 9.2×10^7 s^{-1}, as determined by the measurement of τ^A_{exc}. As illustrated in Figure 9, it results from eq 5 that the nonradiative rate coefficients of conformers B to F vary from $(2.2-3.1) \times 10^7$ to $(6.9-7.8) \times 10^7$ s^{-1} as k^A_{nrad} varies from 0 to 9.2×10^7 s^{-1}. Thus, it appears that k^X_{nrad} (X = B to F) is faster than k^A_{nrad} over half of the $(0-9.2) \times 10^7$ s^{-1} interval where k^A_{nrad} is defined. As a consequence, we cannot definitely conclude whether the nonradiative deexcitation rate of conformer A is higher than those of conformers B to F. Nevertheless, whereas Philips et al.[9] assumed that all conformers had the same radiative lifetime, we propose that all conformers have similar nonradiative deexcitation rate coefficients, centered at 5.4×10^7 s^{-1}.

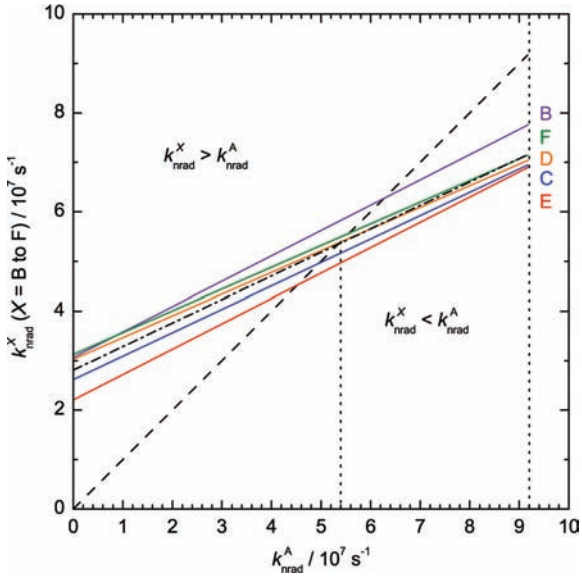

Figure 9. Nonradiative decay rate coefficients k^X_{nrad} of conformers B to F as a function of the nonradiative decay rate coefficient k^A_{nrad} of conformer A. The dashed-dotted line represents the average of the B to F lines. The dashed line ($k^X_{nrad} = k^A_{nrad}$) separates the regions where $k^X_{nrad} > k^A_{nrad}$ and $k^X_{nrad} < k^A_{nrad}$. Vertical dotted lines mark the upper value of k^A_{nrad} (9.2×10^7 s^{-1}) and the value chosen for the calculation of the absolute fluorescence yields (5.4×10^7 s^{-1}), where the average of B to F equals A.

By assuming that the nonradiative deexcitation rate of the vibrationless state S_1 of conformer A takes this value, absolute fluorescence yields can be determined. We find a yield of 0.41 for the vibrationless state of S_1 in conformer A and yields of 0.23 to 0.28 for conformers B to F. In conclusion, conformer A differs from the other conformers by an additional radiative deexcitation process which is the red-shifted fluorescence. This additional process induces a faster deexcitation rate and a higher fluorescence yield for conformer A relative to the other conformers.

Geometry Properties. Rizzo et al.[5] have interpreted the vibrational progression observed in the spectrum of conformer A as being due to a geometry change in the corresponding vibrational coordinate upon electronic excitation. In order to specify the vibrational mode involved, we optimized the geometry of the S_0 state of conformer A and calculated its vibrational modes with the Gaussian software.[29] Both the geometry optimization and the frequency calculation were carried out at the DFT-B3LYP/6-311++G(2d,p) level of theory. The mode of lowest frequency was found to be the torsional motion of Trp about the CC bond connecting the amino acid side chain with the indole chromophore, with each moiety moving relative to the other. This CC bond is indicated by an arrow in Figure 1a. The unscaled calculated harmonic frequency was 29.6 cm^{-1}. By assuming that the vibrational frequencies are similar in the S_0 and S_1 states, this value is to be compared with the 25.5 cm^{-1} band interval of the progression observed in the $S_1 \leftarrow S_0$ transition of conformer A. Given the modest level of theory used in the present study, the calculated frequency and the observed progression are in reasonable agreement, supporting the assignment of the progression to different quanta of excitation of this torsional mode. As a consequence, the geometry change in the corresponding vibrational coordinate postulated by Rizzo et al.[5] can now be specified as a change in the minimum energy angle of the torsional mode upon the $S_1 \leftarrow S_0$ transition. Snoek et al.[8] already optimized the structures of conformer A in the S_1 and S_2 states, which are also labeled ^1L_b and ^1L_a, respectively, in Platt's notation.[30] They reported a difference of ≈3.5° between the values obtained for this angle in the S_0 and $S_2(^1L_a)$ states optimized at the DFT-B3LYP/6-31+G(d) and CIS/6-31G* levels, respectively. They did not report a similar variation between the geometries of the S_0 and S_1 states. Higher-level calculations, relative to CIS/6-31G*, appear to be needed to explore this question further.

Attention is now drawn to the band labeled G in our spectra. We assign it to the origin of the $S_1 \leftarrow S_0$ transition of a new conformer, namely, conformer G. This conformer had not been identified until now because of the lower resolution of the measurements combined with different experimental conditions and detection schemes. Depending on them, the intensity of the bands of conformer A is enhanced relative to the other bands, as can be seen in the spectra of the literature.[5,8] As a consequence, in these spectra, the origin band of G and the nearby A_0^4 band, member of the so-called 26 cm^{-1} vibrational progression, are not separated. A means to overcome this situation is to apply a conformer selection technique such as UV−UV hole burning spectroscopy.[8]

Our assignment of the band to the new conformer G is supported by several arguments. First, by applying a second order polynom to extrapolate the position of A_0^4 from the other band positions of conformer A reported in Table 1, we predict A_0^4 to be at 34 972.00 ± 0.41 cm^{-1}. This value is significantly different from 34 974.23 ± 0.18 cm^{-1}, the measured position of G. Second, in the CRDS spectra, when applying laser vaporization instead of thermal heating, the band is not weakened, unlike those of conformer A. Third, also in the CRDS spectra, the rotational contour exhibits a dip at the top whereas the bands of conformer A are characterized by a single maximum. Finally, band G is stronger than A_0^3, whereas the intensity of A_0^4 is expected to be lower than that of A_0^3.

Besides the A_0^4 and G bands, another band belonging to conformer A is located between those of E and F, as indicated by Snoek et al. in their UV−UV hole burning spectra.[8] This band of conformer A, possibly emphasized by the photoionization-based detection, appears as a small peak in the LIF spectrum in Figure 5b. It is situated at 34 977 cm^{-1}, very close to band F at its low-energy side. Except for the fact that it is due to conformer A, it has yet to be assigned. Thus, the careful comparison of relative band positions in the spectra of Snoek et al.[8] and in our LIF spectrum confirms that the band we have assigned to conformer G cannot be identified with any band of conformer A.

Conclusions

The direct UV absorption spectrum of L-tryptophan cooled in a supersonic jet has been measured for the first time. Applying different vaporization methods, we have observed the advantages of laser vaporization over thermal heating. With laser vaporization, the sample can be heated up to higher temperatures to obtain higher densities in the jet, nevertheless avoiding significant thermal decomposition. In the comparison with thermal heating, the only drawback of the laser vaporization technique is the lower signal-to-noise ratio. This is partly due to the short duration of the vaporization event which limits the accuracy of the measurement of the ring-down time associated with the absorption of Trp.

As for the photophysical properties of Trp, the absorption and LIF spectra show differences in the relative band intensities. We have been able to determine that the fluorescence yield of conformer A is 1.6 times larger than those of the other conformers, due to a strong contribution at red-shifted wave-

lengths, while its intrinsic fluorescence lifetime is twice as short. The red-shifted fluorescence channel therefore appears as a competitor to nonradiative deexcitation channels. Moreover, by proposing that all conformers have a similar nonradiative deexcitation rate, we have determined absolute values for their fluorescence yields.

The geometry of conformer A in its S_0 state has been optimized at the DFT-B3LYP/6-311++G(2d,p) level of theory and the vibrational modes have been calculated. It was found that the lowest-frequency mode in S_0 consists of the torsional motion about the CC bond that connects the amino acid side chain with the indole chromophore. The comparison of this theoretical frequency in S_0 with the vibrational progression observed in the $S_1 \leftarrow S_0$ transition of conformer A indicates that the same mode in S_1 is responsible for the progression. Higher-level calculations would be welcome to confirm that the position of the side chain relative to the chromophore is different in states S_0 and S_1, which would induce the intensity pattern of the observed progression, and to derive theoretical vibronic intensities. These calculations should be carried out for the other conformers as well in order to verify the differences with conformer A.

Because we have used two different vaporization techniques, different distributions of jet-cooled conformers have been produced and observed by absorption spectroscopy. The comparison of the spectra has been instrumental in the assignment of a band to the origin of the $S_1 \leftarrow S_0$ transition of a new conformer, which we have named G. IR-UV hole burning measurements would be helpful to determine the structure of the new conformer. The study of the dependence of the band areas on the temperature could yield information on the internal energy of the different conformers relative to conformer A, and the results could be compared with the calculations of Snoek et al.[8]

Acknowledgment. The authors are grateful to François Piuzzi for communicating R2PI data and details of his laser vaporization source. This work was carried out within a cooperation between the Max-Planck-Institut für Astronomie and the Friedrich-Schiller-Universität Jena. G.R. and F.H. gratefully acknowledge the support of the Deutsche Forschungsgemeinschaft (Project No. Hu474/18). A preliminary account of this work was given during the 26th International Symposium on Rarefied Gas Dynamics.[31]

References and Notes

(1) Kuan, Y.-J.; Charnley, S. B.; Huang, H.-C.; Tseng, W.-L.; Kisiel, Z. *Astrophys. J.* **2003**, *593*, 848.
(2) Snyder, L. E.; Lovas, F. J.; Hollis, J. M.; Friedel, D. M.; Jewell, P. R.; Remijan, A.; Ilyushin, V. V.; Alekseev, E. A.; Dyubko, S. F. *Astrophys. J.* **2005**, *619*, 914.
(3) Jones, P. A.; Cunningham, M. R.; Godfrey, P. D.; Cragg, D. M. *Mon. Not. R. Astron. Soc.* **2007**, *374*, 579.
(4) Cunningham, M. R.; et al. *Mon. Not. R. Astron. Soc.* **2007**, *376*, 1201.
(5) Rizzo, T. R.; Park, Y. D.; Peteanu, L. A.; Levy, D. H. *J. Chem. Phys.* **1986**, *84*, 2534.
(6) Rizzo, T. R.; Park, Y. D.; Levy, D. H. *J. Chem. Phys.* **1986**, *85*, 6945.
(7) Piuzzi, F.; Dimicoli, I.; Mons, M.; Tardivel, B.; Zhao, Q. *Chem. Phys. Lett.* **2000**, *320*, 282.
(8) Snoek, L. C.; Kroemer, R. T.; Hockridge, M. R.; Simons, J. P. *Phys. Chem. Chem. Phys.* **2001**, *3*, 1819.
(9) Philips, L. A.; Webb, S. P.; Martinez, S. J.; Fleming, G. R.; Levy, D. H. *J. Am. Chem. Soc.* **1988**, *110*, 1352.
(10) Teh, C. K.; Sipior, J.; Sulkes, M. *J. Phys. Chem.* **1989**, *93*, 5393.
(11) Rodante, F.; Marrosu, G.; Catalani, G. *Thermochim. Acta* **1992**, *194*, 197.
(12) Bryan, A. M.; Olafsson, P. G. *Anal. Lett.* **1969**, *2*, 505.
(13) Levis, R. J. *Annu. Rev. Phys. Chem.* **1994**, *45*, 483.
(14) Staicu, A.; Rouillé, G.; Sukhorukov, O.; Henning, T.; Huisken, F. *Mol. Phys.* **2004**, *102*, 1777.
(15) Sukhorukov, O.; Staicu, A.; Diegel, E.; Rouillé, G.; Henning, T.; Huisken, F. *Chem. Phys. Lett.* **2004**, *386*, 259.
(16) Rouillé, G.; Arold, M.; Staicu, A.; Krasnokutski, S.; Huisken, F.; Henning, T.; Tan, X.; Salama, F. *J. Chem. Phys.* **2007**, *126*, 174311.
(17) Ralchenko, Y.; Kramida, A. E.; Reader, J. *NIST Atomic Spectra Database (version 3.1.5)*; National Institute of Standards and Technology: Gaithersburg, MD, 2008.
(18) Park, Y. D.; Rizzo, T. R.; Peteanu, L. A.; Levy, D. H. *J. Chem. Phys.* **1986**, *84*, 6539.
(19) Philips, L. A.; Levy, D. H. *J. Chem. Phys.* **1988**, *89*, 85.
(20) Karas, M.; Bachmann, D.; Hillenkamp, F. *Anal. Chem.* **1985**, *57*, 2935.
(21) Hillenkamp, F.; Karas, M.; Holtkamp, D.; Klüsener, P. *Int. J. Mass Spectrom. Ion Processes* **1986**, *69*, 265.
(22) Labazan, I.; Milošević, S. *Chem. Phys. Lett.* **2002**, *352*, 226.
(23) Posthumus, M. A.; Kistemaker, P. G.; Meuzelaar, H. L. C.; de Brauw, M. C. T. N. *Anal. Chem.* **1978**, *50*, 985.
(24) Cable, J. R.; Tubergen, M. J.; Levy, D. H. *J. Am. Chem. Soc.* **1987**, *109*, 6198.
(25) Li, L.; Lubman, D. M. *Rev. Sci. Instrum.* **1988**, *59*, 557.
(26) Ruoff, R. S.; Klots, T. D.; Emilsson, T.; Gutowsky, H. S. *J. Chem. Phys.* **1990**, *93*, 3142.
(27) Huang, Z.; Lin, Z. *J. Phys. Chem. A* **2005**, *109*, 2656.
(28) Short, K. W.; Callis, P. R. *J. Chem. Phys.* **1998**, *108*, 10189.
(29) Frisch, M. J. et al. *GAUSSIAN 03, Revision C.02*; Gaussian, Inc.: Pittsburgh, PA, 2003.
(30) Platt, J. R. *J. Chem. Phys.* **1949**, *17*, 484.
(31) Huisken, F.; Rouillé, G.; Arold, M.; Staicu, A.; Henning, T. *AIP Conf. Proc.* **2008**, *1084*, 539.
(32) Schmitt, M.; Böhm, M.; Ratzer, C.; Vu, C.; Kalkman, I.; Meerts, W. L. *J. Am. Chem. Soc.* **2005**, *127*, 10356.

JP903253S